# Study of H, N, and O atom interaction with quasi-two-dimensional molybdenum disulfide

© *D.E. Melezhenko* [1,2], *D.V. Lopaev* [1], *A.I. Zotovich* [1], *E.N. Voronina* [1,2]

[1] Skobeltsyn Institute of Nuclear Physics, Moscow State University, Moscow, Russia
[2] Moscow State University, Moscow, Russia
E-mail: voroninaen@nsrd.sinp.msu.ru

The paper presents the results of the experimental study of O, N, and H atom interaction with ultra-thin $MoS_2$ films demonstrating changes in properties of the surface layer of samples under investigation.

**Keywords:** quasi-two-dimensional materials, molybdenum disulfide, plasma, ions, surface modification.

Owing to a unique combination of electronic, optical, mechanical, and thermal properties (including high carrier mobility, adjustable bandgap width, etc.), quasi-two-dimensional molybdenum disulfide $MoS_2$ is presently considered to be one of the most promising semiconductor materials for nanoelectronic elements [1–3]. Low-temperature plasma is used widely in the fabrication of electronic elements for etching, doping, surface cleaning, etc. However, active plasma particles (ions and radicals) may cause significant damage to ultrathin materials, thus inducing unwanted changes of both their structure and properties [1,4,5]. Therefore, a thorough analysis of effects induced in such films by both radicals and ions is needed to develop a reliable technology for processing of quasi-two-dimensional materials.

In the present study, the effect of O, N, and H atoms on ultrathin $MoS_2$ films is examined experimentally to identify variations of their structure and optical properties induced in the process, and the specifics of film modification under the influence of low-energy atoms and ions are analyzed.

A test stand with a remote source of inductively coupled plasma (ICP) with a frequency of 13.56 MHz, which was positioned in a quartz tube 84 cm in length with an inner diameter of 16 mm, was used to irradiate $MoS_2$ films with O, N, and H atoms. A flux of O, N, and H atoms, which were produced as a result of dissociation of molecules in passage of $O_2$, $N_2$, and $H_2$ gases through the ICP discharge region (power: 200 W; pressure: 100 mTorr; gas flow: 20 sccm), entered a separate quartz tube (length: 60 cm; inner diameter: 8 cm) that contained the samples. Owing to water cooling of the discharge chamber walls, the probability of recombination of atoms on these walls was reduced considerably. This allowed us to raise the flux density of atoms above the surface of samples. A stainless-steel grid with cells $\sim 70\,\mu$m in size (smaller than the Debye radius for the indicated discharge parameters) was used to prevent the penetration of plasma into the sample chamber. The exposure time varied from 3 to 3600 s.

External circular electrodes were mounted outside the sample chamber to process films with low-energy ions in $O_2$, $N_2$, and $H_2$ plasma and to measure the flux of atoms from the discharge chamber by actinometry. Radio-frequency (RF) power at 81 MHz could be supplied to these electrodes via a matching unit to produce surface-wave discharge. The concentrations of atoms near the surface of samples were measured by differential actinometry with krypton atoms [6]. The flux densities calculated based on these data are listed in the table. The 81-MHz RF power in the process of plasma treatment of films was 10 W. The energy of ions incident on the surface of samples in the course of plasma processing was measured with a grid retarding potential analyzer. The energy spectrum of ions obtained in this context was rather well-peaked with a maximum near the plasma potential ($\sim 22$ eV for $O_2^+$ and $N_2^+$, $\sim 35$ eV for $H_3^+$).

Molybdenum disulfide samples for the experiment were grown by plasma-enhanced chemical vapor deposition on a $SiO_2 + Al_2O_3$ substrate. These samples were examined before and after irradiation *ex situ* using Raman spectroscopy, spectroscopic ellipsometry, X-ray fluorescence (XRF), and X-ray photoelectron spectroscopy (XPS). A spectrometer with a resolution of 2.5 Å based on a Horiba Triax 550 monochromator and an ATC-53-1000 (532 nm) solid-state laser was used to measure Raman spectra. The ellipsometry technique (spectroscopic ellipsometer SENTECH 800 with a wavelength variation range of $300-850$ nm) was used to estimate the thickness of samples and analyze their optical properties. The elemental composition of films and their chemical structure were examined by XPS (Kratos Axis Ultra DLD) and XRF (Oxford Instrument X-act, electron irradiation with an energy of 5 keV).

Raman spectra of the pristine sample in Fig. 1, *a* are characterized by well-marked peaks corresponding to vibrational modes $E_{2g}^1$ and $A_{1g}$. The measured distance between $E_{2g}^1$ and $A_{1g}$ peaks was $\sim 25 \pm 1$ cm$^{-1}$, which yields an estimated minimum $MoS_2$ film thickness of six

Measured concentrations and flux densities of atoms and ions near the surface of samples

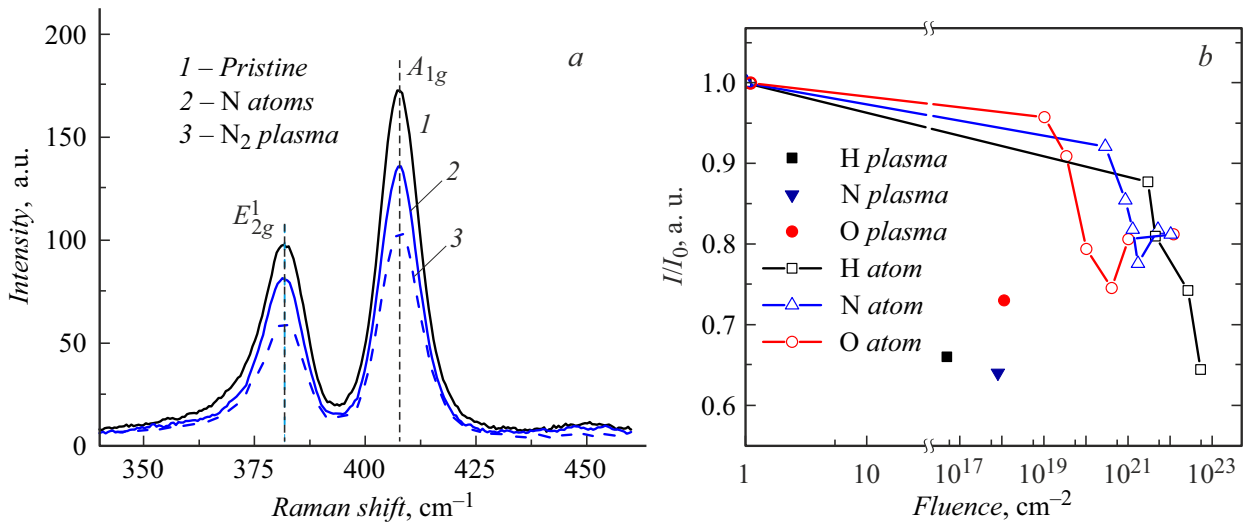| Gas | Particles | Peak energy of ions, eV | Concentration, $10^{10}$ cm$^{-3}$ | Flux density to the sample surface, $10^{14}$ cm$^{-2} \cdot$ s$^{-1}$ |
|---|---|---|---|---|
| O$_2$ | O atoms | − | $2.1 \cdot 10^3$ | $3.3 \cdot 10^3$ |
| | O$_2^+$ ions | 23 | 1.5 | 18 |
| N$_2$ | N atoms | − | $1.7 \cdot 10^3$ | $2.9 \cdot 10^3$ |
| | N$_2^+$ ions | 22 | 0.5 | 6.4 |
| H$_2$ | H atoms | − | $4.5 \cdot 10^3$ | $2.8 \cdot 10^4$ |
| | H$_3^+$ ions | 35 | 0.2 | 7.8 |



**Figure 1.** Raman spectra of pristine and irradiated films ($a$) and dependences of relative intensity $I/I_0$ of peak $A_{1g}$ on the fluence of irradiating particles ($b$).
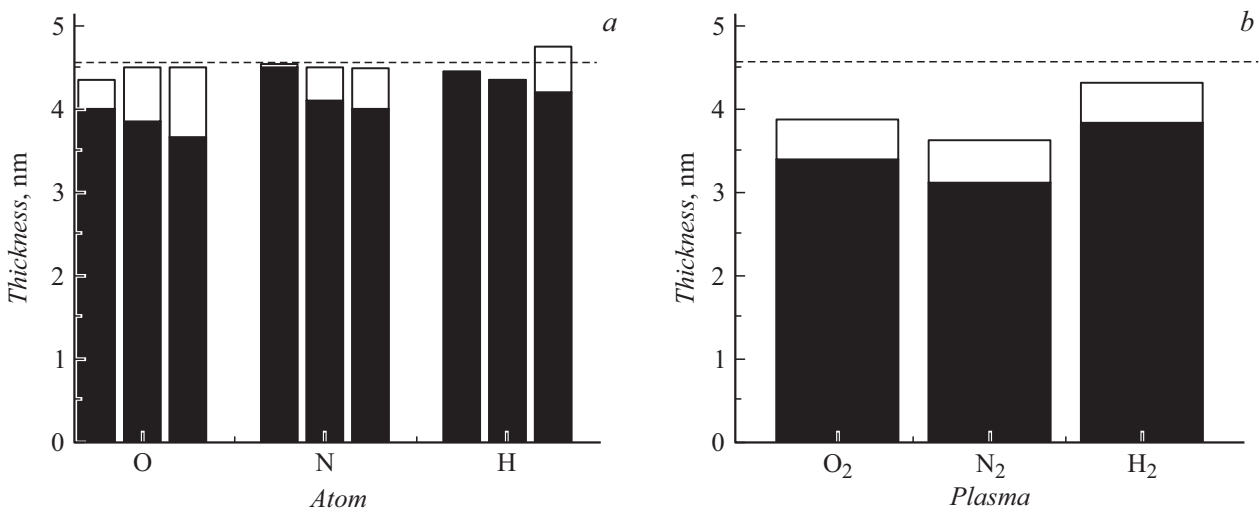


**Figure 2.** Thicknesses of MoS$_2$ films without the substrate determined based on the ellipsometry data after irradiation with: $a$ —atoms at a fluence of $10^{20}$, $10^{21}$, and $10^{22}$ cm$^{-2}$ (left to right); $b$ — ions at a fluence of $\sim 10^{18}$ (N$_2$ and O$_2$ plasma) and $\sim 5 \cdot 10^{16}$ cm$^{-2}$ (H$_2$) plasma. An unperturbed layer of „pure" MoS$_2$ and a modified layer are shown in black and white, respectively; the horizontal dashed line marks the thickness of the pristine film.

monolayers [7]. The general configuration of Raman spectra remained almost unchanged after processing, and no new lines were found. However, the line intensity decreased gradually with increasing processing time. This indicates that the surface $MoS_2$ film layer becomes modified. It can be seen from Fig. 1, $b$ that the line intensity under the influence of plasma (i.e., under irradiation with both ions ans atoms) decreases much faster than in the case of exposure to atoms only. It is important to note that the intensity eventually stops decreasing in the case of processing with O and N atoms, but a similar saturation for H atoms was not observed. This feature may be attributed to the fact that small-sized H atoms penetrate deep into the film and interact with lower-lying layers, while O and N atoms modify only the uppermost monolayer, and this modification ceases at a high dose of irradiating particles.

Spectroscopic ellipsometry was used to examine the influence of irradiation on the optical properties of $MoS_2$ films and estimate their thickness. Since the variations of these properties depend on processing conditions, different optical models containing three basic units (dielectric (substrate) + semiconductor ($MoS_2$ film) + semiconductor/dielectric (modified $MoS_2$ layer) were considered in the analysis of ellipsometric curves. The Cauchy model with a nonzero absorption coefficient and the Tauc−Lorentz model with six oscillators were used for dielectric and semiconductor layers, respectively [8]. The substrate thickness determined for pristine films remained fixed in further analysis. Importantly, the pristine $MoS_2$ film thickness estimated by ellipsometry ($\sim 4.5\,nm$) agrees with the estimate derived from Raman spectra.

The results of application of the mentioned models for estimating the thickness of samples subjected to long-term irradiation are presented in Fig. 2. It follows from the analysis of ellipsometric data that the overall $MoS_2$ film thickness remains almost unchanged under irradiation with atoms (Fig. 2, $a$), although the near-surface optical properties of samples become modified. In the case of N atoms, the model with a semiconducting modified layer with a thickness on the order of one $MoS_2$ monolayer provided the best fit to ellipsometric curves, while the model with a dielectric upper layer (i.e., with a substantially modified upper film layer) was the optimum one after processing with O and H atoms. These models allowed us to compile a consistent description of the emergence and gradual growth of a modified layer with an increase in processing time. It is important to note that this growth in the case of O and N atoms reaches saturation, which correlates well with the dynamics of peak intensities in Raman spectra (Fig. 1, $b$). The model with a semiconducting modified layer was the most efficient for samples after plasma treatment. It demonstrated that the thickness of a $MoS_2$ film irradiated by atoms and ions simultaneously decreases to a more significant extent (Fig. 2, $b$) than in the case of processing with atoms only, and heavy $O_2^+$ and $N_2^+$ ions cause a more intense destruction of upper layers (and subsequent material removal) than light $H_3^+$ ions.
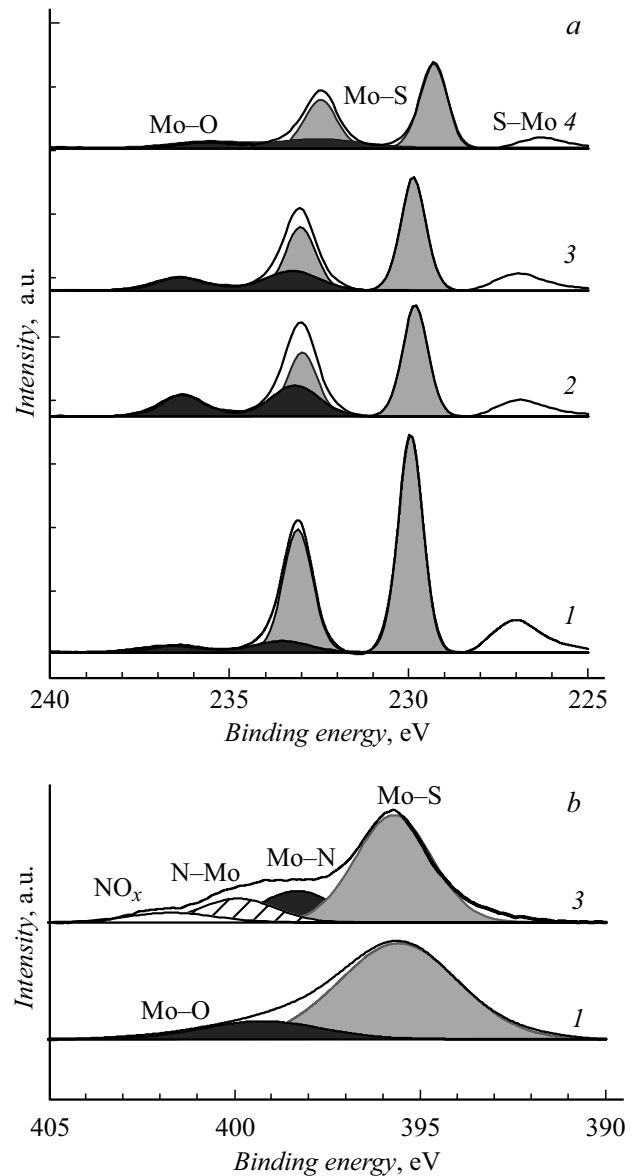


**Figure 3.** High-resolution XPS spectra around $Mo3d_{5/2,3/2}$ peaks with account for spin-orbit splitting ($a$) and N1$s$ and Mo3$p_{3/2}$ peaks ($b$) for the pristine sample ($1$) and samples irradiated with O ($2$), N ($3$), and H ($4$) atoms for 3600 s. Peaks corresponding to Mo−S are colored in gray, Mo−O and Mo−N peaks are black, and the N1$s$−Mo peaks is hatched.

The results of analysis of Raman spectra and ellipsometric data presented below are attributable to the modification of the upper layer of $MoS_2$ films by incident particles. The measured XPS and XRF spectra demonstrated that the concentration of sulfur in samples decreases notably after processing with O and H atoms, while the concentration of oxygen increases. It follows from *ab initio* modeling data [9,10] that vacancies may form in a $MoS_2$ monolayer due to the removal of sulfur under the influence of O and H atoms. These vacancies are filled with oxygen in the process of treatment both in a chamber and in

air, and surface molybdenum oxide $MoO_x$ clusters, which feature dielectric properties, form as a result [11,12]. This mechanism of oxygen implantation into near-surface layers of $MoS_2$ films agrees well with the high-resolution XPS spectra (Fig. 3, $a$): following irradiation with O (curves $2$) and H (curves $4$) atoms, the ratio of intensities of the S2$s$ peak and Mo3$d$ peaks decreased by $25-30\%$, while the Mo$-$O fraction in films increased by a factor of more than $2-3$ (from 0.10 to $\sim 0.34$ for O and $\sim 0.22$ for H). Irradiating N atoms (curve $3$) initiate a similar process that results in the formation of a modified $MoS_xN_y$ layer due to partial substitution of sulfur with nitrogen on the film surface (the ratio of intensities of the S2$s$ peak and Mo3$d$ peaks decreased by $\sim 20\%$ in this case). The features of XPS spectra around 400 eV, where N1$s$ and Mo3$p$ peaks are positioned (Fig. 3, $b$), verified the presence of nitrogen in irradiated samples. Crucially, an ultrathin surface $MoS_xN_y$ layer forming under the influence of N atoms may retain semiconducting properties [13].

Thus, the results of our experiments revealed that the upper layers of ultrathin $MoS_2$ films irradiated with O, N, and H atoms are modified due to the removal of sulfur, the incorporation of incident atoms into newly formed vacancies, and the influence of atmospheric gases. The overall thickness of a film processed with atoms remains almost unchanged, but an ultrathin dielectric layer may form on its surface; owing to their high chemical activity, O atoms alter the properties of near-surface film layers to a more significant extent than N and H atoms. In contrast to atomic irradiation, plasma treatment even at low ion energies results in partial removal of upper layers, thus causing a more intense destruction of films. The obtained data may be used to develop new processing techniques for semiconductor materials and optimize the existing methods.

## Funding

## Conflict of interest

The authors declare that they have no conflict of interest.

## References

[1] Z.M. Wang, *MoS₂: materials, physics, and devices* (Springer, 2014). DOI: 10.1007/978-3-319-02850-7

[2] B. Radisavljevic, A. Radenovic, J. Brivio, V. Giacometti, A. Kis, Nature Nanotechnol., **6** (3), 147 (2011). DOI: 10.1038/nnano.2010.279

[3] L.A. Chernozatonskii, A.A. Artyukh, Phys. Usp., **61** (1), 2 (2018). DOI: 10.3367/UFNe.2017.02.038065.

[4] B.J. Lee, B.J. Lee, J. Lee, J.-W. Yang, K.-H. Kwon, Thin Solid Films, **637**, 32 (2017). DOI: 10.1016/j.tsf.2017.02.014

[5] J. Guo, B. Yang, Zh. Zheng, J. Jiang, Physica E, **87**, 150 (2016). DOI: 10.1016/j.physe.2016.12.004

[6] D.V. Lopaev, A.V. Volynets, S.M. Zyryanov, A.I. Zotovich, A.T. Rakhimov, J. Phys. D, **50** (7), 075202 (2017). DOI: 10.1088/1361-6463/50/7/075202

[7] C. Lee, H. Yan, L.E. Brus, T.F. Heinz, J. Hone, S. Ryu, ACS Nano, **4** (5), 2695 (2010). DOI: 10.1021/nn1003937

[8] G.A. Ermolaev, Y.V. Stebunov, A.A. Vyshnevyy, D.E. Tatarkin, D.I. Yakubovsky, S.M. Novikov, D.G. Baranov, T. Shegai, A.Y. Nikitin, A.V. Arsenin, V.S. Volkov, npj 2D Mater. Appl., **4** (1), 21 (2020). DOI: 10.1038/s41699-020-0155-x

[9] L.M. Farigliano, P.A. Paredes-Oliverab, E.M. Patrito, Phys. Chem. Chem. Phys., **23** (17), 10225 (2021). DOI: 10.1039/D0CP06502A

[10] E.N. Voronina, Y.A. Mankelevich, L.S. Novikov, T.V. Rakhimova, D. Marinov, J.-F. de Marneffe, J. Phys.: Condens. Matter, **32** (44), 445003 (2020). DOI: 10.1088/1361-648X/aba013

[11] K.C. Santosh, R.C. Longo, R.M. Wallace, K. Choet, J. Appl. Phys., **117** (13), 135301 (2015). DOI: 10.1063/1.4916536

[12] M.R. Islam, N. Kang, U. Bhanu, H.P. Paudel, M. Erementchouk, L. Tetard, M.N. Leuenberger, S.I. Khondaker, Nanoscale, **6** (17), 10033 (2014). DOI: 10.1039/C4NR02142H

[13] A. Azcatl, X. Qin, A. Prakash, Ch. Zhang, L. Cheng, Q. Wang, N. Lu, M.J. Kim, J. Kim, K. Cho, R. Addou, Ch.L. Hinkle, J. Appenzeller, R.M. Wallace, Nano Lett., **16** (9), 5437 (2016). DOI: 10.1021/acs.nanolett.6b01853